INVESTIGATION OF MULTIHARMONIC EFFECTS IN A SINGLE STAGE HIGH SPEED COMPRESSOR

M. Amer, N. Maroldt, J. Seume, Institut für Turbomaschinen und Fluid-Dynamik, Leibniz Universität Hannover, An der Universität 1, 30823 Garbsen, Germany

Abstract

Multistage effects in turbomachines can lead to multiresonance phenomena where multiple eigenfrequencies are excited at the same time. In turn, these multiresonance phenomena can result in high amplitude blade vibrations and other as yet uninvestigated phenomena. This results in a shorter fatigue life, and therefore their investigation is of great importance in the prevention of structural failure. Multistage effects result from the reciprocal influence of multiple stages on each other. Multiresonance, a simultaneous excitation of at least two modes, can arise due to different blade numbers in the stages which then lead to an excitation of multiple modes through different engine orders, resulting from the interaction of the number of blades and vanes, simultaneously. To study multistage effects on the vibrational behavior of compressor blisks, a simplified setup is chosen where a single stage blisk is excited by adjustable inlet guide vanes. The multiple stages are represented by changing the angle of attack of each individual vane. This allows the multistage effect to be imitated using adjustable inlet guide vanes. The effect on the blade vibration is measured with a tip timing system. Two major objectives are pursued: firstly, the excitation of two different engine orders, ideally simultaneously, and secondly, the investigation of multistage effects which lead to multiresonance.

Keywords

blisk, compressor, multiharmonic excitation, multistage, engine order, tip timing

1. INTRODUCTION

The prediction of a blade integrated disks (blisks) vibrational behavior is of great interest to ensure safe operation. Blisks are used in turbomachinery as they offer light weight compared to conventional rotors with a bladed disk. The research on blisks is of interest as the blades are characterized by low mechanical damping, which explains why they are easily excited when aerodamping is not present.

Early investigations such as Capece et al. [3] showed the relevance of multistage effects as they investigated a three-stage compressor to characterize the interaction between blade rows excited by aerodynamic effects. They showed that the forcing function is influenced by multiple stages. Murray et al. [8] investigated resonance crossings due to multiple stages of a compressor. They underlined the importance of experimental validation to prove the reliability of numerical tools. The three-stage compressor configuration served as test rig for their experiments in which the first torsional mode was excited and investigated. The necessity of these investigations was also mentioned in connection with rising loads and an increasing demand for blisks in industrial applications. The forced response effects were captured by tip timing which will be also used in this work.

Experiments are always necessary because they indicate mistuning effects which belong to real system behavior but cannot always be captured by numerical methods. Mistuning describes the deviation from a perfectly symmetric structure and has two main effects in turbomachinery [5].

 doi:10.25967/490212

Firstly it changes the air flow and secondly it has an influence on eigenfrequencies and mode shapes. The first effect results from changes in the tip leackage flow and shock position. In turn, this has an impact on the second effect as the described changes cause different pressure fluctuations. The pressure fluctuations have an impact on the aerodynamic damping which leads to shifted eigenfrequencies. These two effects can also have an impact on the lifespan of the whole engine. The low number of existing data sets in the literature emphasizes the need for more accessible research on this topic. Researchers such as Besem et al. [1] conducted a test series and gained a large experimental data set on forced response investigations analyzing single resonance phenomena. Their contribution aimed at answering the unsolved questions in turbomachinery including unsteady effects such as forced response and flutter. They showed that decoupled consideration of several stages is not accurate enough and that the influence of downstream stators is underestimated. Again, mistuning effects were considered and their influence was compared in experimental and numerical data.
Li et al. [7] showed that the influence of the upstream stator is still the dominant reason for the vibrational behavior of the blades. They highlighted the lack of understanding concerning multiple stage interactions.
Heller et al. [4] also used tip timing measurements to characterize blade vibrational behavior in turbomachines which additionally underlines the strength of this measurement technique. Multiharmonic vibration data was captured and modal parameters were determined with a novel global optimization technique.
Bladh et al. [2] investigated multistage coupling of bladed disks. They underlined the necessity for accurate treatment of interstage effects. These multistage effects can result in changed modal blade-disk interaction. Mistuning effects were also considered in these investigations. They suggested taking multiple stages into account when the excitation frequency is close to eigenfrequencies.
Recent literature on multistage effects thus focuses on structural mechanics and aerodynamic disturbances from upstream vanes and rotor stages leading to forced response in compressors. Multiresonance, however, has yet not been investigated. The investigation in the present work therefore focuses on two objectives:

1. Multiharmonic excitation – excitation of two engine orders (EO) in a speed range as small as possible
2. Multiresonance – simultaneous excitation of two modes

2. METHOD

2.1. Multiharmonic excitation

To understand the physical principles behind multiharmonic excitation, experiments were conducted on the high speed axial compressor test rig of the Institute of Turbomachinery and Fluid-Dynamics (TFD). A single stage rotor with a blisk consisting of 24 blades is used. This configuration consists of an adjustable inlet guide vane (IGV) with 23 vanes together with an adjustable stator downstream with 27 vanes. The number of inlet guide vanes (23) results in exciting the first engine order. This engine order is always present. The vanes' angle of attack can be adjusted within a range of $\pm 20°$. The vanes are illustrated in Fig. 1. The flow direction is from bottom right to top left, the vane row on the right representing the IGV. Downstream of the IGV the stator row is located.

To excite the single stage blisk with more than one engine order, the second engine order is introduced by adjusting a certain number of inlet guide vanes in a defined angle. Two methods will be:

- Method 1: Only certain vanes are rotated in an angle of $10°$ (in this case with 6 vanes).
- Method 2: All vanes are rotated in angles between $0°$ and $20°$ in $2°$ steps to represent a sine wave around the circumference.

An adjustment scheme for Method 2 to excite EO6 is shown in Fig. 2. Figure 2 shows the optimized positions for each vane to excite EO6, which will be explained below. The dots on the sine wave represent the 23 vanes. The y-axis shows the angle of the vanes between $0°$ and

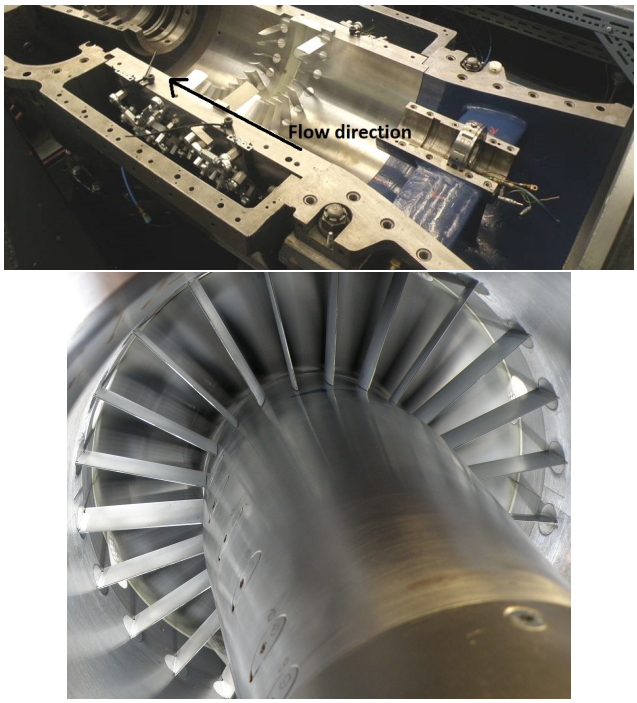

Figure 1: IGV

$20°$. While a synchronous rotation of all vanes could be performed automatically, the adjustment of individual vanes has to be done by hand.
To ensure the success of the excitation mechanism, a circumferential mode analysis is carried out. This method is developed in aeroacoustics where the sound pressure is transformed into complex circumferential modes. In this method, a discrete Fourier transform (DFT) is applied to provide the amplitude and phase of the pressure spectrum [6]. It can thus be detected which orders will excite the system through the pressure distribution. A virtual pressure distribution is constructed, initially with Method 1. The pressure amplitude is assumed to scale with the angle of the adjustment, which is a simplification used to facilitate investigating the excitation. This distribution is shown in Fig. 3, where the virtual dimensionless pressure represents the changed flow field downstream of the IGV due to the adjusted vanes. The changes in the flow field result from the increased wake size.
The 6 adjusted vanes each generate a peak, and all other vanes with an angle of $0°$ correspond to the value zero. The 6 peaks are not equally spaced as there is no even partition due to the 23 vanes. The Fourier transform subsequently performed on the virtual pressure distribution shown in Fig. 3 highlights which order will lead to an elevated excitation. The result is presented in Fig. 4. Engine order 6 shows a higher peak compared to other orders, and it can be expected that Method 1 will excite EO6 and thus corresponding blade vibrations can be measured in operation. Another high peak can be seen for engine order 23, due to the asymmetric distribution of the 6 adjusted vanes, therefore an additional excitation at EO23 can be expected through Method 1.
The same procedure can be carried out for the sinusoidal pattern of the vane angles (Method 2). The virtual pressure distribution is again deduced from the adjustment pattern of the vanes. The sine wave is visible in the virtual pressure distribution in Fig. 5. Figure 6 shows the results of the DFT performed on the sound pressure distribution shown in Fig. 5. It also indicates that both EO6 and EO23 have a strong impact on the blade vibration. The amplitudes of the sinusoidal pattern are about two times higher than those resulting from Method 1. Compared to Method 1 no significant excitation of other harmonics next to order 6 can be observed. The peaks of other orders are a lot lower compared to the ones in Fig. 4. The difference is due to the shape of the pressure distribution which in this case is closer to the sine wave. This could lead to distinct excitation of the orders 6 and 23 which will be investigated. However, a verification based upon real measurement data is necessary.
The first 5 eigenmodes and their normalized deflections are displayed in Fig. 7. These mode shapes were generated from a numerical modal analysis of the blades with fixed boundary conditions at the blade root using ANSYS Mech. 19.1. The mode shapes 2 and 4 have their highest deflection at the blade leading edge. Unfortunately, due to design restrictions, the tip timing probes, which will measure the vibrational behavior are located close to the trailing edge of the blade tip (see section 2.2). Therefore, modes 2 and 4 can not be considered as options for studying multiresonance effects. Although mode 1 has its highest deflection at the leading edge, the deflections at the trailing edge are still high enough to be detected by the tip timing system. In addition, the first mode usually has the overall highest deflections compared to modes of higher order which further explains why it can be de-

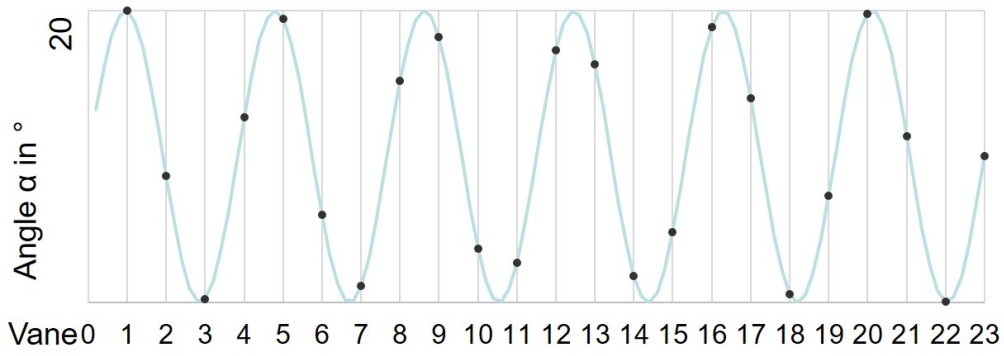

Figure 2: Optimized positions for each vane (Method 2)

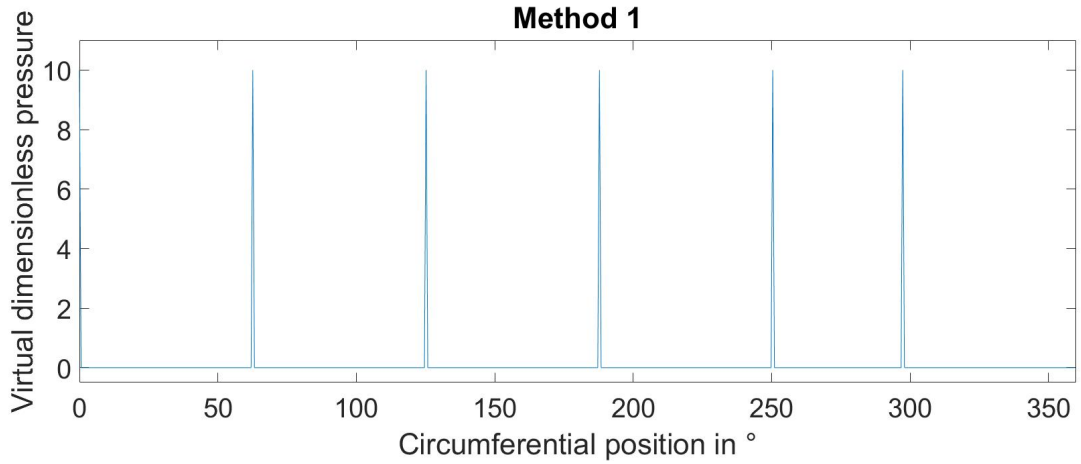

Figure 3: Virtual dimensionless pressure distribution for Method 1

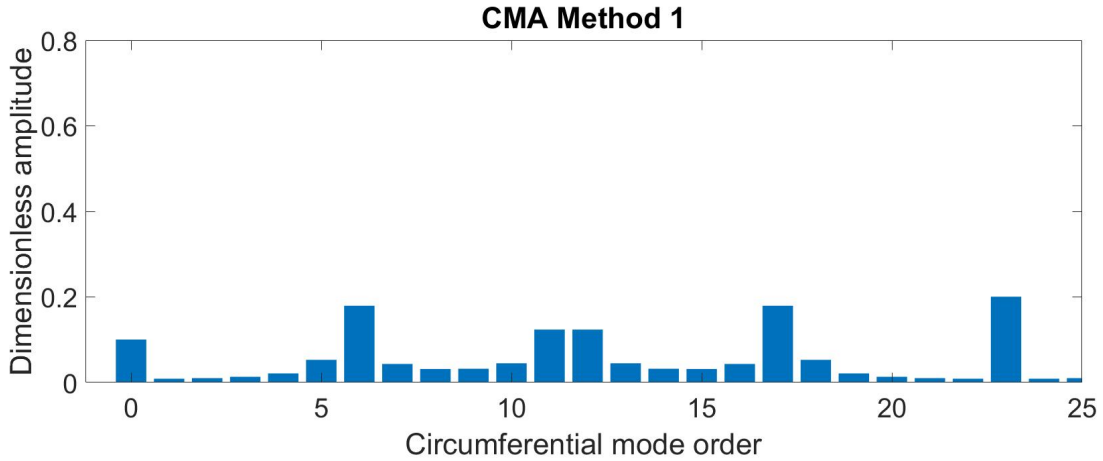

Figure 4: Circumferential mode analysis of Method 1

tected properly. Mode 1 is easily excited by the system and small environmental disturbances and as such, it serves well as an eigenmode being part of the multiresonance effect. Modes higher than eigenmode 5 are not considered below as their maximum amplitude is presumed to be within the measurement uncertainty of the tip timing system, and thus can not be properly detected.

The Campbell diagram of the blisk is shown

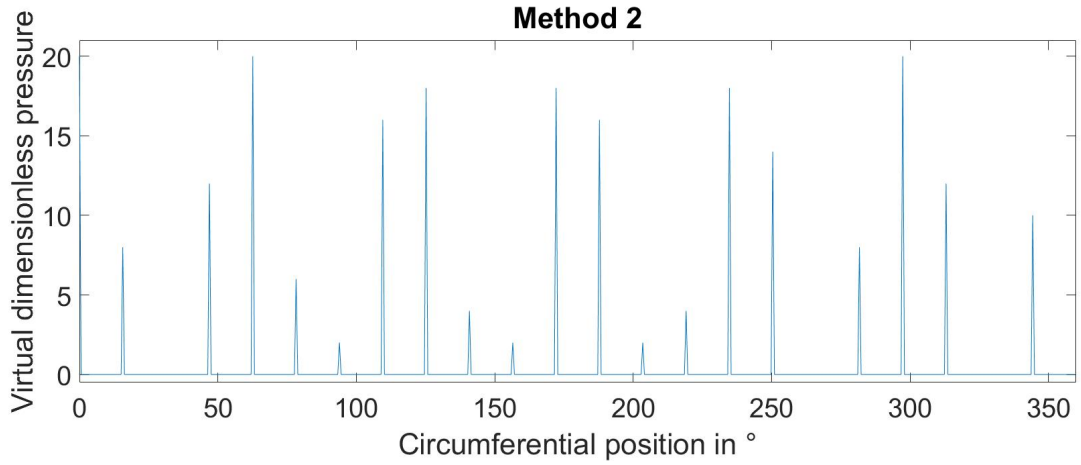

Figure 5: Virtual dimensionless pressure distribution for Method 2

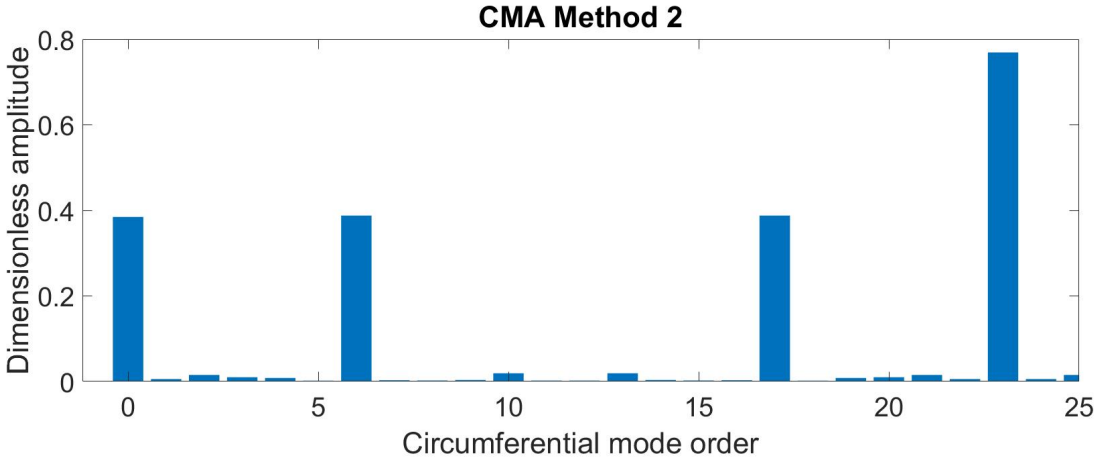

Figure 6: Circumferential mode analysis of Method 2

in Fig. 8. By means of this diagram it can be detected, where two engine orders lead to multiresonance. According to the explanation above, the focus will be on the excitation of modes 1, 3, and 5. The objective of analyzing the Campbell diagram is to find theoretical rotational speeds where two different modes have an intersection point with EO23 and another one below 23. The second engine order has to be smaller than 23 as the set up provides only 23 inlet guide vanes. A rotational speed found from this analysis should lead to multiresonance in operation. The results of this first analysis are shown by the dashed green lines in the Campbell diagram 8. The Campbell diagram is derived from modal analysis data of the blisks' full cyclic model. The first possible rotational speed is determined as 6615 rpm, where mode 1 excited by EO6 and mode 3 excited by EO23 can lead to multiharmonic excitation. The second option for multiharmonic excitation is found at 14870 rpm where mode 1 is excited by EO3 and mode 5 by EO23. These two options are summarized in table 1.

1. EO	1. Mode	2. EO	2. Mode	Δf
6	1	23	3	46.5 Hz
3	1	23	5	39 Hz

Table 1: Options of multiharmonic excitation

It must be acknowledged that nonetheless there is a deviation between the frequencies of the predicted and experimentally observed resonance peak. The difference between the resonance peak of mode 1 and mode 3 is 46.5 Hz, the difference between the resonance peak of mode 1 and mode 5 is 39 Hz. Before conducting the ex-

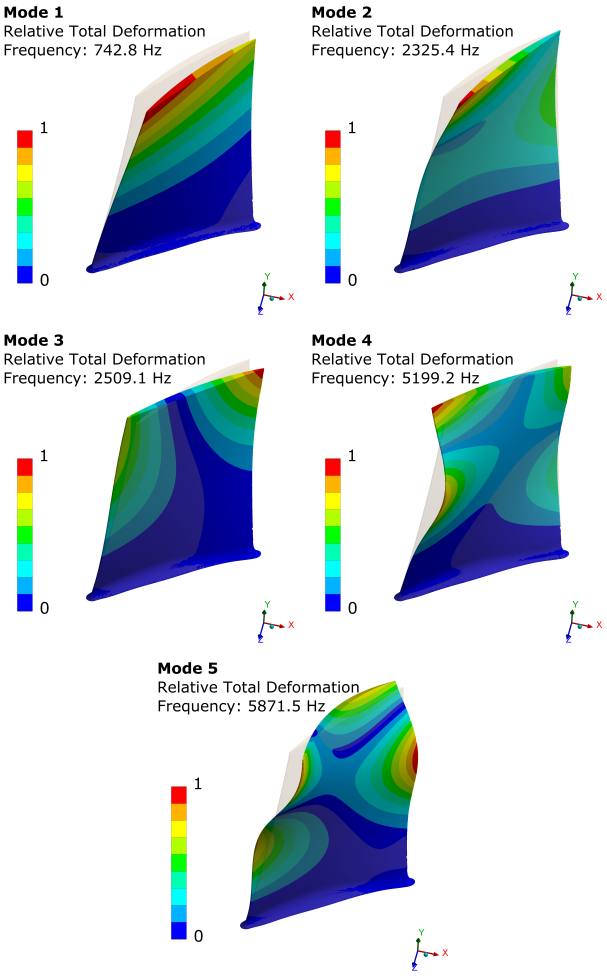

Figure 7: Mode shapes 1 - 5

periments it is not known how the vibrational behavior is influenced by real flow conditions and how the fading curve of each resonance will look resulting in a maximum range where two modes are still excitable simultaneously. This mainly depends on the max. amplitude and the damping of the excited mode. The options in Table 1 result in a testing schedule with two operating points considered in the experiments. Below the first option with EO6 and EO23 will be explored. To investigate this point of interest, engine order 6 needs to be physically present in the system. Method 1 is applied with six vanes adjusted with an angle of $10°$. The adjustment scheme for Method 2 can be extracted from Fig. 2.

2.2. Instrumentation and data acquisition

To perform the measurements, a tip timing system by Agilis is used. It consists of eight laser probes, mounted in the casing pointing to the rotor blade trailing edge. These tip timing probes measure the time of arrival (TOA) of each blade. The TOA is a reference for the delay of the blade due to blade vibration. Knowing the TOA and the circumferential position of the probes, as well as a given Campbell diagram allows the excited eigenmode to be calculated, as well as other important parameters like aerodamping.
Transients are being carried out in operation of the axial compressor to collect the essential data with the measurement system. The transient operational behavior is necessary in order to capture the forced response effects. For this purpose the rotational speed is increased slowly during the measurement. From the transient curves, the resonance effects can be derived. They occur at the amplitude peaks shown in Fig. 9. The amplitudes are visible because they are present next to the rotational speed regions where no mode excitation is taking place. These transients can take place in a range of 3000 rpm up to the nominal speed of 17100 rpm.

3. RESULTS

To study the effect of multiharmonic excitation, the tip timing results are analyzed. Fig. 9 displays the amplitude of each rotor blade detected by an exemplary tip timing probe. It captures a tran-

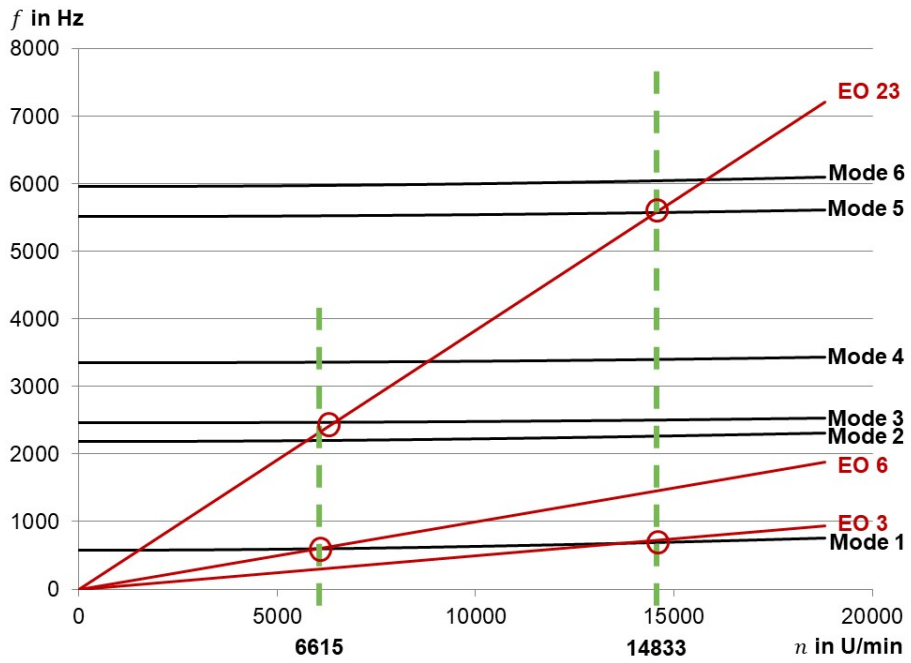

Figure 8: Campbell diagram

sient speed line starting approximately with 6000 rpm running up to 6700 rpm. The increase in rotational speed is shown by the red straight line. The blade deflection is displayed over time respectively increasing rotational speed. The analysis of Fig. 9 results in two clear peaks. The first higher and broader peak belongs to EO6 exciting mode 1 and is displayed at approximately 6136 rpm. The second peak belongs to EO23 exciting mode 3 at approximately 6634 rpm. Fig. 9 already shows that the second objective of exciting two modes simultaneously is not achieved at this operating point. The two resonance peaks are too far away from each other and no overlap between mode 1 and mode 3 can be observed.

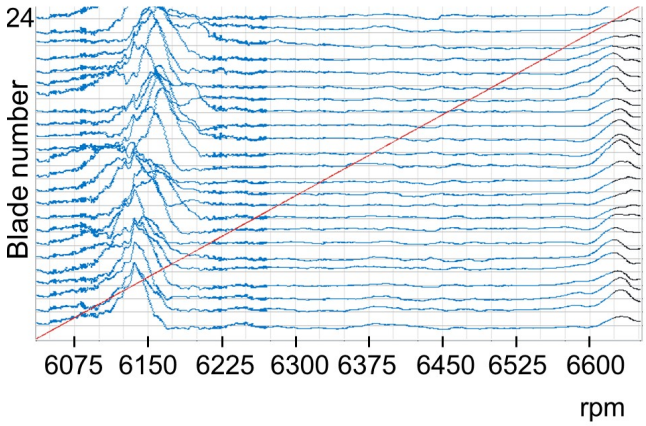

Figure 9: Deflection of each rotor blade (supplementary excitation of EO6)

For further analysis, the averaged blade amplitudes are displayed in the Campbell diagram in Fig. 10. The results are calculated for EO6 and EO23 using the least-square fit model. The first 4 modes are illustrated by gray straight lines over a rotational speed range between 6000 and 7000 rpm. The green curve fitted over the mode displays the blade deflection. The green color corresponds to a good data fit of approximately 100 % with respect to a model of EO6 fitted into the data by the analysis algorithm and EO23 for mode 3 respectively shows what frequency distance between two peaks is still within acceptable bounds to detect multiharmonic excitation. The difference in frequency between a first significant increase of the amplitude and the peak of mode 1 is approx. 15 Hz. The same applies to the distance between peak and end of the fading curve as the resonance behavior is nearly symmetric. The deviation of the peaks belonging to mode 3 is approx. 12 Hz. Unfortunately, the calculated difference between those two resonance peaks thus is approximately 3 times higher than the acceptable maximum allowable deviation previously identi-

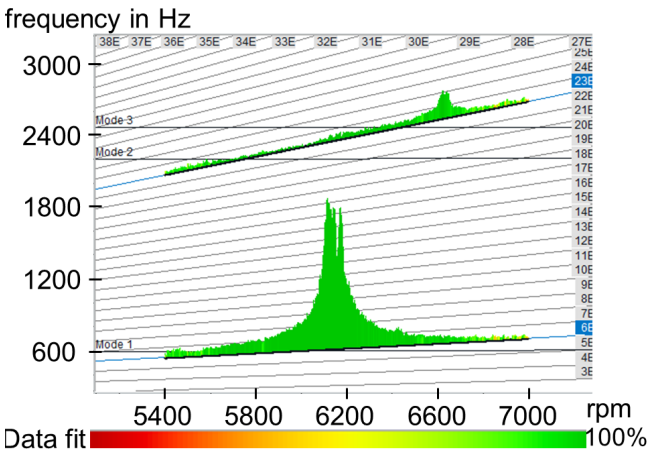

Figure 10: Averaged blade deflection plotted over the Campbell diagram (supplementary excitation of EO6)

fied in experiments observing multiresonance effects. In conclusion, the start of the second resonance needs to deviate less than 12 Hz for multiresonance to occur. A simultaneous excitation of mode 1 and mode 3 by the determined engine orders is thus not possible. As the deviation in table 1 for the second option (EO3 and EO23) corresponds still to 39 Hz, a simultaneous excitation of mode 1 and mode 5 will not be observed in operation either. This particularly applies as it is likely that the difference between start of resonance and peak is going to decrease with rising modes. Fig. 11 proves this assumption as the two peaks can be detected next to each other. Fig. 11

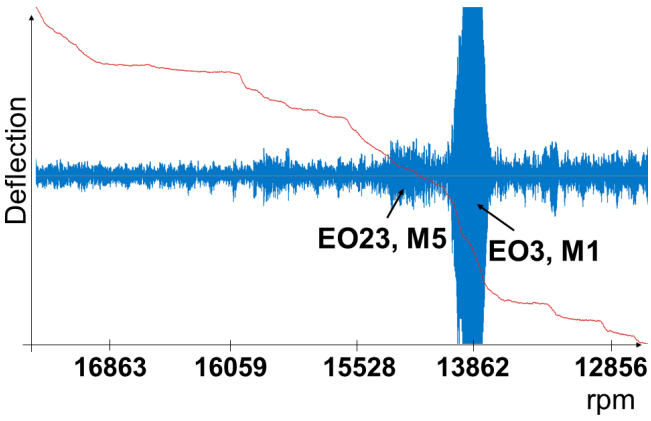

Figure 11: Blade deflection of an examplary blade (supplementary excitation of EO3)

shows a run-down of rotational speed (red line) and an exemplary blade signal. Each blade signal is similar, such that findings for one blade can be applied to all other rotor blades. The resonance for mode 5 excited by EO23 takes place at approximately 14896 rpm. The resonance for mode 1 excited by EO3 occurs at approximately 13862 rpm. Figure 11 shows that the elevated amplitudes of the resonance are next to each other and thus do not cause multiresonance. As it was assumed above, 39 Hz deviation in frequency is too high to ensure multiresonance.

However, the first objective of this work which is the excitation of multiple modes in general can still be investigated. Fig. 9, 10, and 11 show a dominant peak for EO6 and EO3 which are forced upon the system by the different schemes. In conclusion, the excitation of a second engine order through adjustment of the IGV is carried out successfully.

However, the predicted multiharmonic excitation can not be accomplished with the present compressor configuration. Two alternatives can be named to achieve multiharmonic excitation. The first one is to change the tip timing positions so that mode 2 and mode 4 become part of the investigation. Other excitation possibilities can then be explored in the future. The second alternative is an adapted blisk design which offers at least one operating point of multiresonance with the existing instrumentation.

As a next step, the influence of the excitation mechanism (Method 1 vs. Method 2) is analyzed. The excitation of EO6 serves as an example for the following conclusions. The resulting amplitudes of both methods at the resonance peak are compared in Fig. 12. The first bar shows the averaged amplitude of the rotor with no adjustment of the inlet guide vanes (all vanes have an angle of $0°$). The value corresponds to 59 μm. The highest amplitude can be observed for Method 2. The amplitude resulting from Method 1 corresponds to 290 μm, whereas Method 2 leads to an averaged vibration amplitude of 1140 μm. Method 2 seems to be a powerful excitation pattern for EO6. This is presumable due to a targeted excitation of EO6 by the sinusoidal pattern. These results highlight the large effect of the upstream stator vanes on the vibrational behavior of the rotor blades.

The main result derived from Fig. 12 is the high

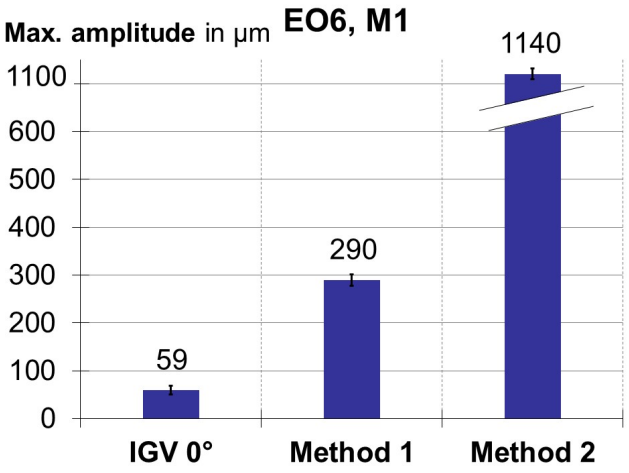

Figure 12: Averaged blade deflection of mode 1

increase of amplitude for Method 2. The amplitude for the sinusoidal excitation pattern is nearly 4 times higher than the amplitudes resulting from the excitation through Method 1. The amplitude resulting from Method 1 in turn is nearly 5 times higher than the amplitude without any defined excitation.

4. CONCLUSIONS AND OUTLOOK

Multiharmonic effects are investigated experimentally specifically for multiresonance in a high speed axial compressor equipped with a single stage blisk and adjustable vanes upstream and downstream of the rotor. The numerically predicted multiresonance could not be achieved in operation. A separation of 15 Hz for mode 1 and 12 Hz for mode 3, respectively appears to be the maximum separation by which two resonance peaks can lie apart from each other, based upon the shape of the fading curve. However, the excitation mechanism itself could be verified as increase in amplitude could be observed for both methods explored.
The gathered experimental data will be used in future work to improve the numerical model which was used to predict multiresonance and serve as boundary conditions for numerical aerodynamic and aeroelastic simulations. Further investigations move the tip timing measurement positions to the blade leading edge in such a way that mode 2 and 4 can also be explored for possible multiresonance.

ACKNOWLEDGEMENTS

The results are gained within the research project C6 “Aeroelasticity of Multistage Axial Compressors“ funded by the Deutsche Forschungsgemeinschaft (DFG, German Research Foundation) – SFB 871/3 – 119193472. The authors kindly thank DFG for the financial support to accomplish this research project.

References

[1] Fanny M Besem, Robert E Kielb, Paul Galpin, Laith Zori, and Nicole L Key. Mistuned forced response predictions of an embedded rotor in a multistage compressor. *Journal of Turbomachinery*, 138(6), 2016.

[2] R Bladh, MP Castanier, and Christophe Pierre. Effects of multistage coupling and disk flexibility on mistuned bladed disk dynamics. *J. Eng. Gas Turbines Power*, 125(1):121–130, 2003.

[3] VR Capece, SR Manwaring, and S Fleeter. Unsteady blade row interactions in a multistage compressor. *Journal of Propulsion and Power*, 2(2):168–174, 1986.

[4] D Heller, IA Sever, and CW Schwingshackl. A method for multi-harmonic vibration analysis of turbomachinery blades using blade tip-timing and clearance sensor waveforms and optimization techniques. *Mechanical Systems and Signal Processing*, 142:106741, 2020.

[5] Christian Keller, Andreas Kellersmann, Jens Friedrichs, and Joerg R Seume. Influence of geometric imperfections on aerodynamic and aeroelastic behavior of a compressor blisk. In *ASME Turbo Expo 2017: Turbomachinery Technical Conference and Exposition*. American Society of Mechanical Engineers Digital Collection, 2017.

[6] Olaf Lemke. Aktive minderung des drehklangs einer axialen fanstufe mittels drucklufteinblasung in den blattspitzenbereich. 2014.

[7] Jing Li, Nyansafo Aye-Addo, Nicholas Kormanik III, Douglas Matthews, Nicole Key, and Robert Kielb. Mistuned higher-order mode forced response of an embedded compressor rotor: Part iâsteady and unsteady aerodynamics. In *Turbo Expo: Power for Land, Sea, and Air*, volume 50930, page V07BT36A021. American Society of Mechanical Engineers, 2017.

[8] William L Murray III and Nicole L Key. Experimental investigation of a forced-response condition in a multistage compressor. *Journal of Propulsion and Power*, 31(5):1320–1329, 2015.